Dipolar and quadrupolar freezing in (NaCN)1−x(KCN)x

Alois Loidl, T. Schräder, R. Böhmer, K. Knorr, J. K. Kjems, R. Born

Angaben zur Veröffentlichung / Publication details:

Loidl, Alois, T. Schräder, R. Böhmer, K. Knorr, J. K. Kjems, and R. Born. 1986. "Dipolar and quadrupolar freezing in (NaCN)1−x(KCN)x." *Physical Review B* 34 (2): 1238–49. https://doi.org/10.1103/physrevb.34.1238.

Dipolar and quadrupolar freezing in $(NaCN)_{1-x}(KCN)_x$

A. Loidl, T. Schräder, R. Böhmer, and K. Knorr
Institut für Physik der Universität Mainz, Postfach 3980, D-6500 Mainz, West Germany

J. K. Kjems
Risø National Laboratory, DK-6400 Roskilde, Denmark

R. Born
Institut für Kristallographie, Universität Tübingen, D-7400 Tübingen, Federal Republic of Germany
(Received 13 February 1986)

$(NaCN)_{1-x}(KCN)_x$ mixed crystals with concentrations $x=0.85$ and 0.59 have been investigated by elastic and inelastic neutron scattering, x-ray diffraction, and dielectric techniques. Both crystals exhibit neither quadrupolar nor dipolar long-range order down to the lowest temperatures. However, the slowing down of the dipolar and the quadrupolar relaxation behaves very differently in the two samples investigated. In $(NaCN)_{0.15}(KCN)_{0.85}$ the freezing-in of the quadrupolar degrees of freedom is a cooperative effect which is dominated by strain-mediated interactions. The resulting low-temperature state is characterized by frozen-in orientational correlations and frozen-in lattice strains. In $(NaCN)_{0.41}(KCN)_{0.59}$ the experimental results on the dynamics of the quadrupolar freezing are indicative of single-ion behavior where the slowing down of the molecular reorientations is completely due to thermal activation across the hindering barriers of the crystal field set up by the neighboring Na^+ and K^+ ions. Consequently the low-temperature state for $x=0.59$ is characterized by quenched quadrupolar disorder, i.e., independently frozen-in single CN^- ions. An analysis of the static dielectric susceptibilities demonstrates that dipolar interaction forces are negligible in $(NaCN)_{0.41}(KCN)_{0.59}$ while significant deviations from a Curie-type behavior exist in $(NaCN)_{0.15}(KCN)_{0.85}$ indicating the onset of short-range electric order near 70 K.

I. INTRODUCTION

The alkali cyanide alkali halide mixed crystals $(KBr)_{1-x}(KCN)_x$ (Ref. 1), $(KCl)_{1-x}(KCN)_x$ (Ref. 2), and $(NaCl)_{1-x}(NaCN)_x$ (Ref. 3) show fascinating (x,T) phase diagrams. The room-temperature structure is the NaCl type, with the CN^- molecules being rotationally disordered. In these high-temperature phases the CN^- ions undergo fast reorientations. At low temperatures a rich variety of crystallographic phases exhibiting orientational and electric long-range order has been reported.[1-5] The elastic phase transitions are triggered by a linear coupling of the quadrupolar relaxations, i.e., the reorientations of the aspherical CN^- molecules, to the lattice strains. However, over wide concentration ranges these crystals remain in a quadrupolar disordered state with frozen-in random CN^- orientations and frozen-in lattice strains. Due to a weak dipole moment of the CN^- molecule (0.3 D) the dipolar relaxation is only a secondary process following the primary relaxation kinetics which is characterized by a cooperative freezing of the quadrupolar degrees of freedom.[6] The onset of the low-temperature quadrupolar frozen-in state is signaled by anomalies in the temperature dependence of the quadrupolar susceptibilities[6-13] which show striking similarities with the spin-glass transition.[14] In addition, it has been found that the low-temperature thermodynamic,[15-17] ultrasonic,[18] and dielectric[16] properties are analogous to those found in canonical glasses and in amorphous solids.[19-21] At present, enormous theoretical efforts are being undertaken to describe this low-temperature state in the framework of orientational,[22,23] quadrupolar,[24] Potts,[25] or canonical[17,26] glasses. The first theoretical approach showing that strain defects in alkali halides can produce a glassy low-temperature state has been outlined by Fischer and Klein.[27]

Recently, it has been shown that $(NaCN)_{1-x}(KCN)_x$ mixtures exhibit an orientationally disordered, low-temperature state in a concentration range $0.15 \leq x \leq 0.89$.[28] This is an unexpected result as the pure cyanides, NaCN and KCN, respectively, show two consecutive phase transitions where the CN^- ions undergo an elastic and an electric ordering process. An (x,T) phase diagram, as experimentally determined by Lüty and Ortiz-Lopez,[28] is shown in Fig. 1. The shaded areas mark the regions of elastic order; the antiferroelectric transition temperatures for the pure cyanides are also indicated. The steep decrease of the phase-boundary lines with the alkali-metal substitution is a remarkable feature of this phase diagram. Already, a 10-at.% substitution of the potassium ions by sodium ions and vice versa suppresses the elastic and the electric order.

In KCN and NaCN the CN^- molecules are surrounded by alkali-metal ions in an octahedral symmetry. In this cubic crystal field the CN^- ions perform reorientational jumps between equivalent symmetry directions. These reorientational excitations are coupled to the translational modes driving the elastic phase transition.[29-32] Obviously, in $(NaCN)_{1-x}(KCN)_x$ the substitution of the large K^+

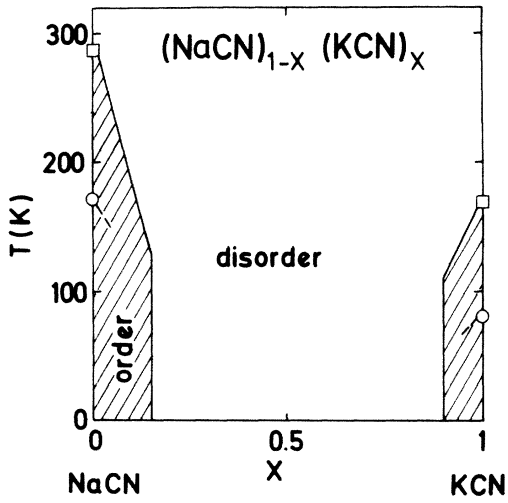

FIG. 1. Approximate (x,T) phase diagram of $(NaCN)_{1-x}(KCN)_x$ after Lüty and Ortiz-Lopez (Ref. 28). The hatched areas indicate the elastically ordered regions. For the pure cynanides the phase-transition temperatures into the elastically (□) and electrically (○) ordered states are indicated.

ions ($r=1.33$ Å) by the smaller Na^+ ions ($r=0.98$ Å) introduces a strong disturbance of the crystalline field, thereby effecting the rotation-translation coupling and changing the dipolar and the quadrupolar relaxation kinetics, which culminates in the fact that these crystals do not show ferroelastic ordering despite a 100-at.% CN^- concentration.

In this paper we present a detailed experimental investigation of $(NaCN)_{1-x}(KCN)_x$ crystals with concentrations $x=0.85$ and 0.59 using x-ray- and neutron-scattering techniques as well as dielectric measurements. Both crystals investigated stay cubic down to the lowest temperatures and exhibit neither a quadrupolar nor a dipolar long-range-ordered state of the CN^- molecules. However, we found that the two samples behave rather differently: The 85-at.% crystal shows a strong rotation-translation coupling. The freezing, as measured in an inelastic-neutron-scattering experiment at THz frequencies, occurs at $T=100$ K. At this temperature the shear modes have almost completely softened and the low-temperature state exhibits frozen-in orientational correlations and frozen-in lattice strains very similar to the findings in $(KBr)_{1-x}(KCN)_x$ with a concentration $x=0.5$.[7] $(NaCN)_{0.41}(KCN)_{0.59}$ exhibits a much weaker coupling of the molecular reorientations to the translational excitations, giving only a weak-strain-mediated interaction between neighboring CN^- molecules. In addition, the freezing sets in at higher temperatures, indicating higher barriers against quadrupolar relaxation. The shear modes undergo no significant softening and, consequently, the freezing-in is, in the first respect, a single-ion phenomenon and the low-temperature state is only a weakly disturbed cubic fcc lattice.

In the neutron-scattering experiments no indications of long-range electric order could be detected for $x=0.59$ or for $x=0.85$. The dielectric measurements, however, indicated that for $(NaCN)_{0.15}(KCN)_{0.85}$ the static dipolar susceptibility deviates from a Curie-type behavior, as expected for noninteracting CN^- dipoles. Obviously, in this crystal dipolar interaction forces contribute to the dipolar freezing-in process and establish short-range electric order for $T \lesssim 70$ K.

II. EXPERIMENTAL DETAILS AND RESULTS

The crystals have been grown at the Crystal Growth Laboratory of the University of Utah using the Kyropoulos technique starting from zone-refined KCN and NaCN. The composition of the melt for the two crystals investigated was $x=0.75$ and 0.5. The actual concentrations were determined at the University of Utah using atomic-absorption spectrophotometry.

The quality of the crystals was investigated using x-ray- and neutron-scattering diffraction techniques. $(NaCN)_{0.15}(KCN)_{0.85}$ was a high-quality single crystal with a mosaic spread of less than 20′. The $(NaCN)_{0.41}(KCN)_{0.59}$ crystal was of minor quality, showing a rocking curve with a full width at half maximum of 2° including a number of misoriented grains. However, at room temperature both crystals exhibited unambiguously a single-domain rocksalt structure with lattice constants $a=6.390$ Å ($x=0.85$) and 6.235 Å ($x=0.59$). We could not detect any decomposition due to a miscibility gap. The occurrence of a miscibility gap at concentrations near $x=0.5$ has been reported by Truthe[33] in an early calorimetric investigation of KCN:NaCN mixtures.

A. X-ray diffraction

Powders were prepared by grinding pieces of single crystals of $(NaCN)_{1-x}(KCN)_x$. The powders then were sprayed onto a Si(100) wafer and held in place by soaking them with a small amount of vacuum grease. The platelet was attached to the cold plate of a closed-cycle refrigerator which was equipped with a Be cylinder allowing the passing of the x rays. The x rays emerged from a Cu tube operated at 40 kV and 20 mA. A graphite monochromator was set to reflect the K_α component (1.542 Å). The powder spectra were measured using a flat position-sensitive detector. In the geometry chosen, the detector spanned an arc of approximately 20° in the scattering angle 2θ. Each sample was investigated at different detector settings.

Figures 2 and 3 show typical results at higher scattering angles, demonstrating the temperature dependence of the (331), (420), and (422) Bragg reflections for both samples investigated. At room temperature, well-defined Bragg peaks were detected. In $(NaCN)_{0.41}(KCN)_{0.59}$ these cubic powder lines are well defined at all temperatures. However, for the concentration $x=0.85$ an enormous temperature-dependent increase of the linewidth becomes apparent. The broadening of the linewidth is strongly momentum-transfer dependent. At low temperatures and high scattering angles the spectra show no clear Bragg peaks. The analysis of the scattering-angle dependence of the linewidth $\Delta\theta$ yields some information concerning the origin of the observed broadening effect.[34] According to fragmentation theories, particle-size effects yield an in-

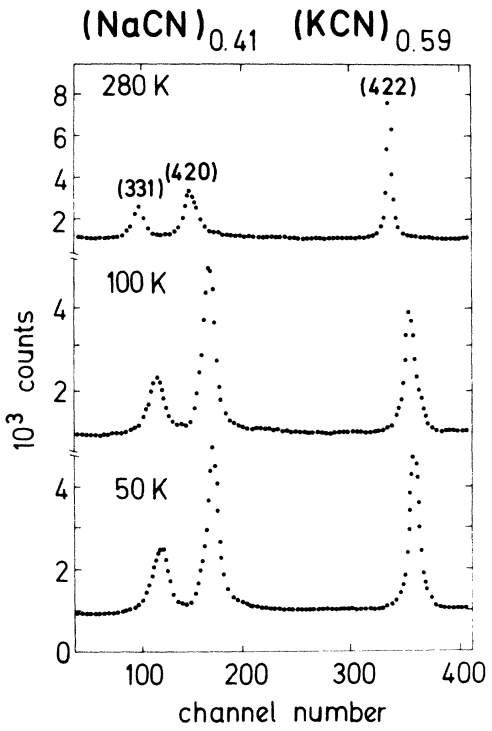

FIG. 2. Parts of the powder spectra of $(NaCN)_{0.41}(KCN)_{0.59}$ as determined by x-ray diffraction, displaying some cubic fcc powder lines at three temperatures. One channel equals 0.04° in 2θ.

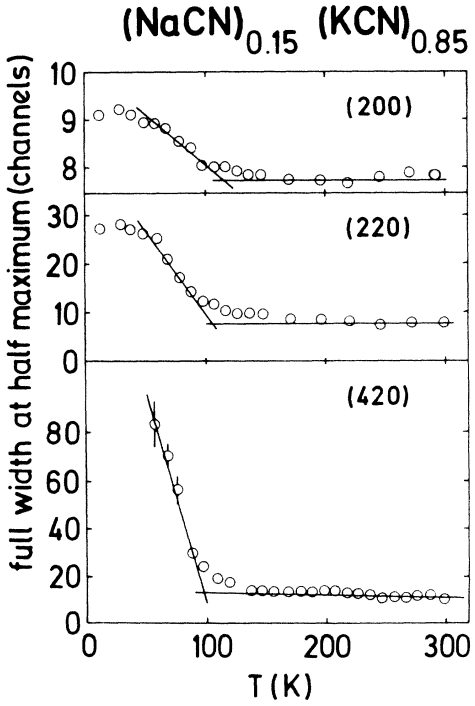

FIG. 4. Temperature dependence of the apparent width of selected powder lines in $(NaCN)_{0.15}(KCN)_{0.85}$ measured by x-ray techniques.

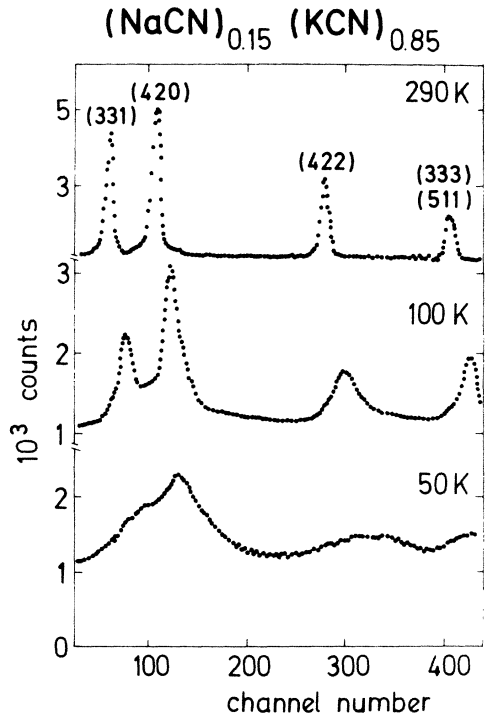

FIG. 3. Parts of the x-ray powder spectrum of $(NaCN)_{0.15}(KCN)_{0.85}$ displaying the extreme broadening of the cubic powder lines with decreasing temperatures. One channel equals 0.04° in 2θ.

crease of the linewidth like $\Delta\theta \propto 1/\cos\theta$ which is not observed in the present x-ray experiment. A distribution of lattice parameters around an average pattern produces an increase of the linewidth according to $\Delta\theta \propto \tan\theta$. This seems to be a more adequate description of the experimental results and could be explained through the onset of random strains centered around zero strain. This distribution of frozen-in random strains introduces a distribution of lattice parameters around the cubic lattice of the high-temperature phase. At present, single-crystal diffraction studies are performed to study this line-broadening effect in more detail. From the present results we conclude that at temperatures below 50 K the scattered intensities are indicative for a sample with no long-range order. These results are similar to the results as obtained in $(KBr)_{0.47}(KCN)_{0.53}$.[34] A summary of the x-ray results in $(NaCN)_{0.15}(KCN)_{0.85}$ showing the strong scattering-angle-dependent broadening of the diffraction lines is given in Fig. 4. The breakdown of true long-range order appears at 100 K. The width of the diffraction lines, a direct measure of the distribution of random strains, increases steadily as the temperature is lowered further.

B. Neutron diffraction

Powders prepared from the same single crystals used in the x-ray study have been investigated by neutron diffraction also. These experiments were carried out at the multidetector diffractometer R 1 located at the thermal neu-

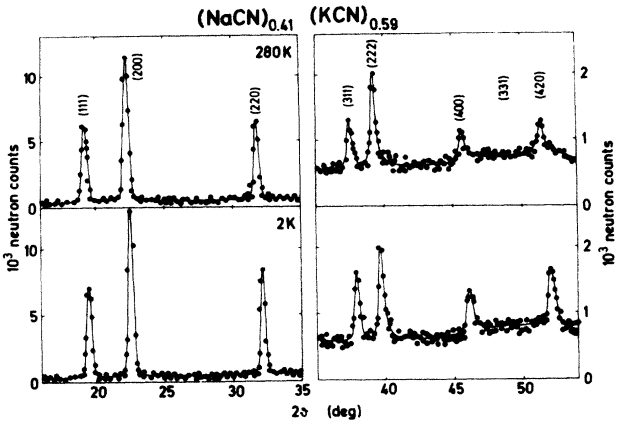

FIG. 5. Observed neutron-diffraction pattern for $(NaCN)_{0.41}(KCN)_{0.59}$ at 280 and 2 K. The solid line is only a guide to the eye. Note the change of scales in the second half of the spectra.

tron source of the BER II reactor at the Hahn-Meitner-Institut für Kernforschung, Berlin, with an incident-neutron wavelength $\lambda = 1.21$ Å. The results are shown in Figs. 5 and 6. Again, as in the x-ray experiments, the well-defined diffraction lines of a cubic fcc lattice can be observed in $(NaCN)_{0.41}(KCN)_{0.59}$ at all temperatures. Due to the form factor of the CN^- ions, the scattered intensities at higher momentum transfers are weak and the (331) reflection is undetectably small. For $(NaCN)_{0.15}(KCN)_{0.85}$ the diffraction pattern for temperatures $T < 100$ K show large contributions due to thermal diffusive scattering processes which increase with decreasing temperatures. At $T = 2$ K large and anomalous, broad quasielastic intensities in addition to the Bragg lines are indicative of frozen-in lattice strains. However, even at the largest scattering angles, well-defined Gaussian contributions due to Bragg scattering are superimposed onto the quasielastic

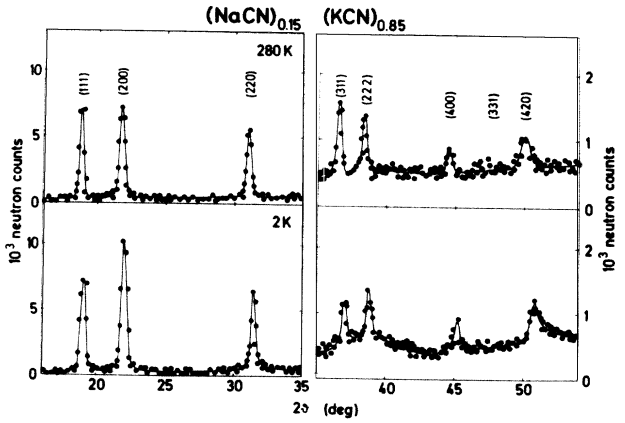

FIG. 6. Observed neutron-diffraction pattern for $(NaCN)_{0.15}(KCN)_{0.85}$ at 280 and 2 K. The solid line is only a guide to the eye. Note the change of scales in the second half of the spectra.

scattered intensities, contrary to the findings in the x-ray experiments.

In both samples no extra peaks due to an ordering of the CN^- molecules with respect to head and tail could be detected. From the neutron-scattering results we can exclude any phase transition into a low-temperature state exhibiting long-range elastic or electric order.

At present, we can offer no explanation for these observed differences in the x-ray and neutron powder spectra. However, one should keep in mind that the x rays probe the alkali-metal ions K^+ and Na^+, while the scattered neutrons, in the wave-vector region investigated, are sensitive to the positions of the CN^- sublattice. Both results could be explained assuming that only the alkali-metal sublattice has lost long-range translational order, while the center-of-mass sublattice of the CN^- molecules still occupies the cubic lattice sites of the high-temperature phase.

C. Inelastic-neutron-scattering investigations

The inelastic-neutron-scattering experiments were performed on a triple-axis spectrometer located at the cold-neutron source of the DR3 reactor at the Risø National Laboratory. All the scans were performed in the (011) scattering plane with the constant-Q mode of operation. The outgoing energy was held constant at 5 meV ($\lambda = 4.05$ Å). To avoid higher-order contaminations, a cooled beryllium filter was used. The collimation was 60′ before and after the monochromator and analyzer crystals.

In these experiments we followed the temperature dependence of the neutron groups as measured at $q/q_{ZB} = 0.1$ (ZB denotes zone boundary) in the [100]TA branch with a sound velocity proportional to the elastic constant c_{44}. Some raw data for $(NaCN)_{0.41}(KCN)_{0.59}$ and $(NaCN)_{0.15}(KCN)_{0.85}$ are shown in Figs. 7 and 8. In the crystal with a potassium concentration of $x = 0.59$, a nearly-temperature-independent neutron group is located at $\hbar\omega = 0.55$ meV. A slight increase of the narrow central line is detectable as the temperature is decreased. The crystal with a concentration $x = 0.85$ exhibits a very different behavior. From room temperature down to 100 K the neutron group as measured along [100]TA undergoes a considerable softening, passes through a minimum, and increases again as the temperature is lowered further. For $T < 100$ K the scattered-neutron line shapes are broadened and a dominant narrow central line appears. The linewidth of this central peak is determined by the resolution of the spectrometer at all temperatures. The findings in $(NaCN)_{0.15}(KCN)_{0.85}$ are very similar to the data collected in $(KBr)_{0.5}(KCN)_{0.5}$.[7] Here the growth of the central line was related to the temperature behavior of the order parameter of an orientational glass phase.[22]

Figure 9 shows a scan through the (111) Bragg reflection at low and high temperatures. As deduced from these measurements, the full width at half maximum is temperature independent within the experimental error. However, strong thermal diffuse intensities appear at low temperatures, corresponding to the central line in Fig. 7. The quasielastic line exhibits a significant asymmetry, in-

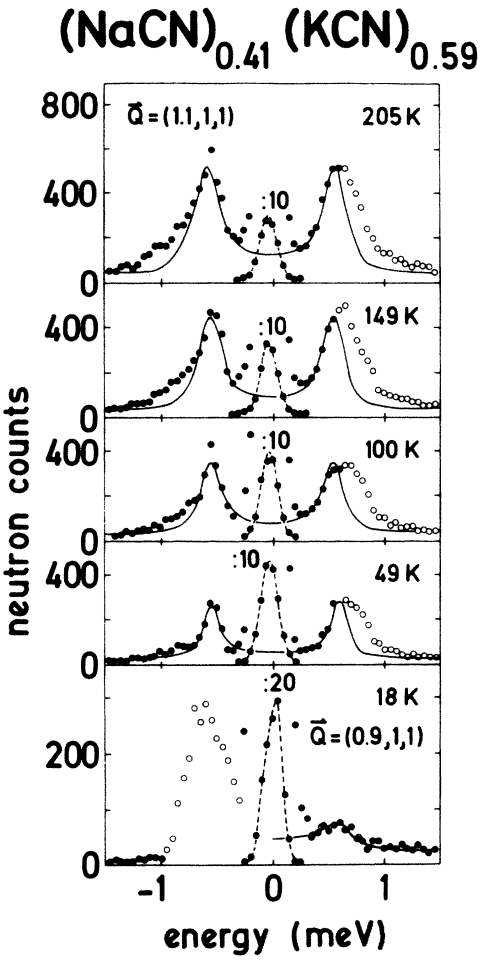

FIG. 7. Neutron-scattering line shapes in T_{2g} symmetry in $(NaCN)_{0.41}(KCN)_{0.59}$ at different temperatures. The solid lines are results of fits of a relaxational model to the experimentally observed line shapes. The open symbols indicate the regions where excess intensity is picked up from the (111) Bragg reflection as a result of the finite resolution.

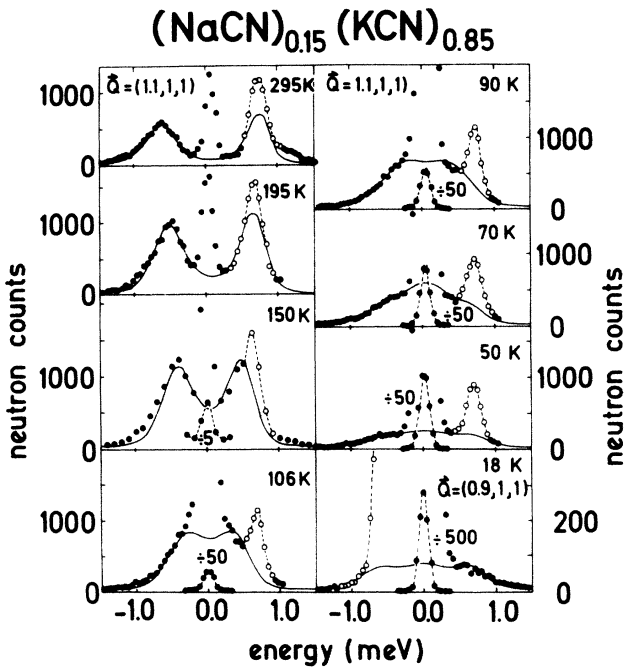

FIG. 8. Neutron-scattering line shapes in T_{2g} symmetry in $(NaCN)_{0.15}(KCN)_{0.85}$ at different temperatures. The solid lines are results of fits of a relaxational model to the experimentally observed line shapes. The open symbols indicate the regions where excess intensity is picked up from the (111) Bragg reflection as a result of the finite resolution.

dicative of a bilinear coupling of rotations and translations.[22]

In order to analyze the experimental data, we fitted the observed neutron line shapes using a pseudospin approach in the relaxational limit as developed by Silverman.[35] The resulting model is very similar to that derived from a microscopic approach by Michel *et al.*[22,29,30] and by Sahu and Mahanti.[32] It has already been successfully applied to coupled rotational and translational excitations in $(KBr)_{1-x}(KCN)_x$ (Ref. 13) and CsCN (Ref. 36). In this approach the quadrupolar susceptibility $\chi(\omega)$ in the relaxational limit is given by[35]

$$\chi(\omega)=\frac{1}{k_BT}\frac{1}{1+i\omega\tau}\ , \tag{1}$$

where ω is the measuring angular frequency and τ is the relaxation time. The pseudospin susceptibility can be coupled to the translational excitations via the one-phonon propagator

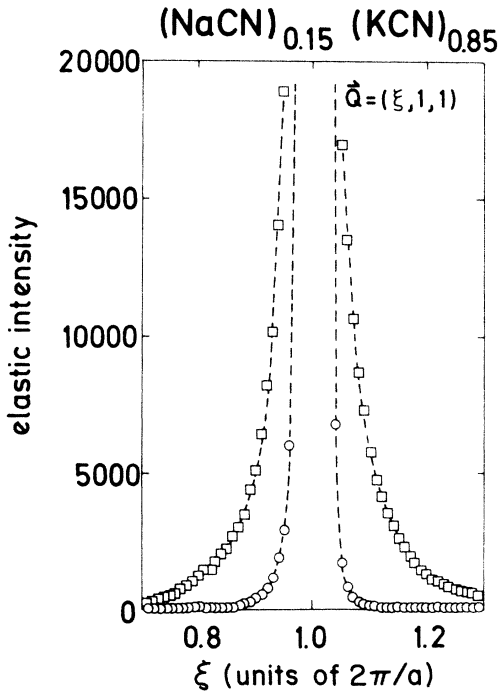

FIG. 9. Quasielastic scan through the (111) Bragg reflection in $(NaCN)_{0.15}(KCN)_{0.85}$ at room temperature (○) and at 18 K (□). Only the lower part of the scattered intensities is shown. The full width at half maximum is temperature independent within the experimental error.

TABLE I. Parameters T_S and Γ determined from the fits of the relaxational model to the observed neutron line shapes in $(NaCN)_{1-x}(KCN)_x$ along [100]TA. $(\hbar\omega)^2$ was kept fixed at 0.46 meV ($x=0.59$) and 0.64 meV ($x=0.85$).

x	T (K)	T_S (K)	$\hbar\Gamma$ (meV)
0.85	295	100±10	1.5 + 0.2
	250	90	1.5
	195	100	1.5
	160	100	1.9
	130	100	1.5
	106	80±10	1.0
	90	65±5	0.9
	70	48	0.7 + 0.2
	50	30±5	0.6 + 0.1
	18	10±2	0.6 + 0.1
0.59	295	55±5	1.5 + 0.2
	205	55	1.5
	149	55	1.5±0.2
	100	40±5	1.5±0.3
	18	7±2	0.5±0.2

$$D(\mathbf{q},\omega)=\frac{2\omega_0(\mathbf{q})}{\omega_0^2(\mathbf{q})[1-k_BT_S\chi(\omega)]-\omega^2}\,. \tag{2}$$

Here, ω_0 is the undisturbed quasiharmonic frequency of a given translational mode with wave vector $\mathbf{q}$ which is decoupled from the rotational excitations. k_BT_S is the rotation-translation coupling. For small phonon wave numbers the coupling is proportional to ω_0^2.[13,32] The intensity of the central line, which is a direct measure of the order parameter of the glass state,[22] is an extra feature of the scattered-neutron line shapes and cannot be explained within the framework of the relaxational model.

Only three relevant parameters enter into the fitting procedure; namely, the undisturbed phonon frequency ω_0, the relaxation rate $\Gamma=1/\tau$, and the rotation-translation coupling k_BT_S. The solid lines in Figs. 7 and 8 are the results of these fits. The parameters as deduced from the analysis are given in Table I. The quasiharmonic phonon energy $\hbar\omega_0$ was estimated from a fit to the sound velocities as determined from the temperature dependence of the centers of the observed neutron groups and then kept fixed. This will be discussed later in more detail. In the temperature range $300<T<100$ K and for $x=0.85$, the rotation-translation coupling ($T_S=95$ K) and the relaxation rate ($\hbar\Gamma=1.5$ meV) are temperature independent. For $T\lesssim 100$ K, T_S and Γ decrease. The decrease of the rotation-translation coupling indicates that now the majority of the CN^- ions relax too slowly to respond within the time window of the neutron-scattering experiment. However, the decrease of the coupling constant T_S and the relaxation rate Γ are too smooth and far too small compared to the temperature dependence of a thermally activated reorientation process over the hindering barrier of the crystal field. A broad distribution of relaxation times could explain the experimentally observed behavior.

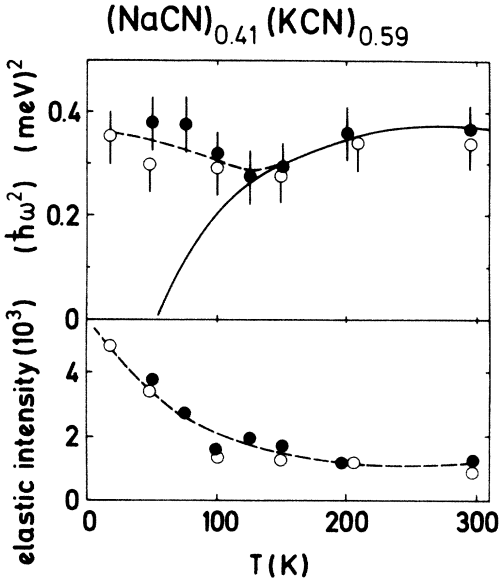

FIG. 10. Squared phonon frequencies and quasielastic scattered intensities at $\mathbf{Q}=(1.1, 1, 1)$ versus temperature, displaying the freezing process in $(NaCN)_{0.41}(KCN)_{0.59}$. The solid line is a fit of a Curie-Weiss law to the experimental data points. The dashed line is a guide to the eye only. Different symbols refer to different experimental setups.

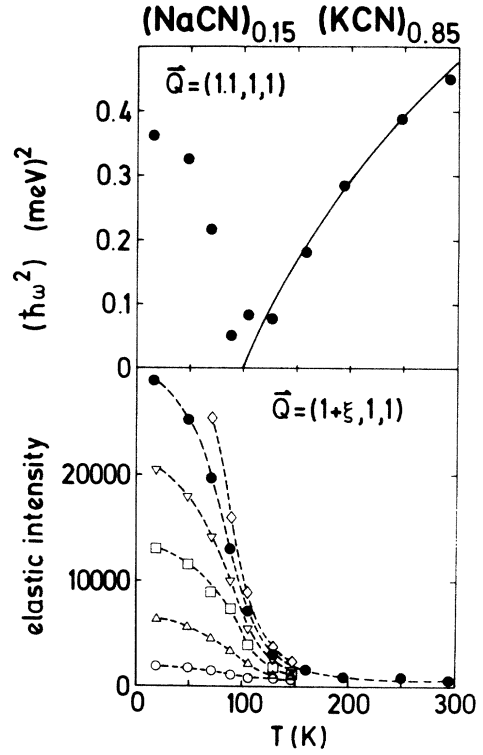

FIG. 11. Upper part: squared phonon frequencies as measured at $\mathbf{Q}=(1.1, 1, 1)$ in $(NaCN)_{0.15}(KCN)_{0.85}$ versus temperature. The solid line represents a Curie-Weiss fit. Lower part: quasielastic intensities measured along $(1+\xi, 1, 1)$ at different temperatures. $\xi=0.075$ (◇), 0.1 (●), 0.12 (▽), 0.15 (□), 0.2 (△), and 0.3 (○). The dashed lines are guides to the eye only.

Similar effects, although much less pronounced, were detected for $(NaCN)_{0.41}(KCN)_{0.59}$.

A summary of these measurements, namely the temperature dependence of the squared phonon energies which is a measure of the elastic constant c_{44} and of the intensities of the central line of all scans along [100]TA, is shown in Figs. 10 and 11. For both concentrations the sound velocity passes through a minimum ($x=0.85$, $T=100$ K; $x=0.59$, $T=130$ K). The effect is easily detectable in $(NaCN)_{0.15}(KCN)_{0.85}$, while it is within the error bars for $x=0.59$. Equally strong differences appear in the increase of the intensities of the central line. However, in both samples the quasielastic intensities appear at the temperature of the minimum sound velocities and increase as the temperature is lowered further. In Fig. 11 the wave-vector dependence of the central line is also indicated.

The solid lines in Figs. 10 and 11 show the results of fits of a Curie-Weiss law to the temperature dependence of the elastic constants c_{44} using

$$c_{44}=c_{44}^{0}(T-T_S)/(T-T_C)\ . \tag{3}$$

The rotation-translation coupling $k_B T_S$ gives the fictitious transition temperature T_S, where c_{44} would vanish if the phase transition is of second order. T_C is the clamped transition temperature. Here the molecules would order in the absence of the rotation-translation coupling. T_C includes direct electric interactions and indirect interactions mediated via optical phonons.[32] With $T_C=0$, Eq. (3) can be deduced from the poles of the denominator of Eq. (2), and this formalism has been used to determine the quasiharmonic phonon frequencies in the analysis of the scattered-neutron line shapes.

The parameters of these fits using Eq. (3) are listed in Table II, together with the parameters obtained in KCN (Ref. 37) and NaCN (Ref. 38). Table II shows that the rotating-translation coupling in $(NaCN)_{1-x}(KCN)_x$ is a factor of 2 smaller for $x=0.59$ compared to $x=0.85$. At present, the very small value of the elastic background constant c_{44}^{0} cannot be explained. It is interesting to note that for the $x=0.59$ sample the fit yields a clamped transition temperature T_C of approximately 0 K, which means that the quadrupolar molecular susceptibility follows a Curie law. However, we have to admit that the fit for $x=0.59$ relies essentially on six data points and the resulting values of c_{44}^{0} and T_c should not be taken too seriously.

TABLE II. Parameters as determined from a fit of a Curie-Weiss law to the temperature dependence of the squared phonon frequency measured at $q/q_{ZB}=0.1$ along [100]TA at temperatures $T>T_F$. The parameters for the pure cyanides were taken from Refs. 37 (KCN) and 38 (NaCN).

x	c_{44}^{0} (10^{10} dyn cm^2)	T_S (K)	T_C (K)
1	5.24	151	−230
0.85	4.5±0.2	100±5	−220±30
0.59	1.6±0.2	55±5	0±30
0	9.5	262	−694

From the analysis of the x-ray and neutron data we conclude that $(NaCN)_{0.15}(KCN)_{0.85}$ exhibits a strong rotation-translation coupling which is, however, somewhat lower than in pure KCN. The transition into an elastically long-range-ordered state is prevented by a freezing-in of the CN^- ions. The onset of strong quasielastic scattering at the freezing temperature T_F shows that, analogous to $(KBr)_{0.5}(KCN)_{0.5}$, this freezing process is a cooperative phenomenon establishing orientational short-range order[22] and destroying the translational long-range order of the center-of-mass lattice.[34] In $(NaCN)_{0.15}(KCN)_{0.85}$ the contribution of the single-ion crystalline anisotropy to the effective hindering barriers is still small. The freezing is driven by the quadrupolar interaction forces,[6,39] but the Na^+ defect concentration is high enough to suppress long-range orientational order. In $(NaCN)_{0.41}(KCN)_{0.59}$ the rotation-translation coupling is further weakened and the freezing-in process starts already at higher temperatures, indicating higher hindering barriers against molecular reorientations. In this mixed crystal the high hindering barriers are due to the strong anisotropy of the crystal field created by the substitution of K^+ through Na^+ ions with a concentration of approximately 50 at. %. The strongly noncubic crystalline field forces the CN^- molecules locally into preferred orientations and, consequently, the quadrupolar freezing is predominantly a single-ion phenomenon. At low temperatures we find randomly quenched CN^- orientations.

D. Dielectric investigations

Using inelastic-neutron-scattering techniques we probed the dynamic quadrupolar susceptibility of the CN^- molecules. From elastic neutron diffraction we know that no electric long-range order is established in the two samples investigated. To gain some insight into the dynamics of the dipolar freezing, we performed dielectric measurements. Real and imaginary parts of the dielectric constant were recorded automatically using a multifrequency LCR meter in a frequency range 100 Hz $<\nu<$ 100 kHz. Some representative results of the frequency and temperature dependence of the dielectric constant $\epsilon'(\nu)$ and the dielectric loss $\epsilon''(\nu)$ are shown in Figs. 12–14. With decreasing temperatures, the dipolar relaxation slows down, resulting in dispersion in the real and a loss peak in the imaginary part of the complex dielectric constant $\epsilon(\nu)$. The maximum in the dielectric loss appears at $\omega\tau=1$ defining the temperature, where the molecular relaxation rate $1/\tau$ equals a given measuring angular frequency ω. Figure 12 shows the temperature dependence of the real part of the dielectric constant ϵ' in $(NaCN)_{0.41}(KCN)_{0.59}$ for different measuring frequencies. The competing contributions of a $1/T$ Curie term of the static dielectric susceptibility and the decrease of $\epsilon'(\nu,T)$ due to dispersion effects give well-defined cusps which are shifted to lower temperatures with lower measuring frequencies. Similar results were observed in $(NaCN)_{0.15}(KCN)_{0.85}$. However, in this crystal no well-defined $1/T$ dependence of ϵ' was detectable at temperatures above the dispersion regime.

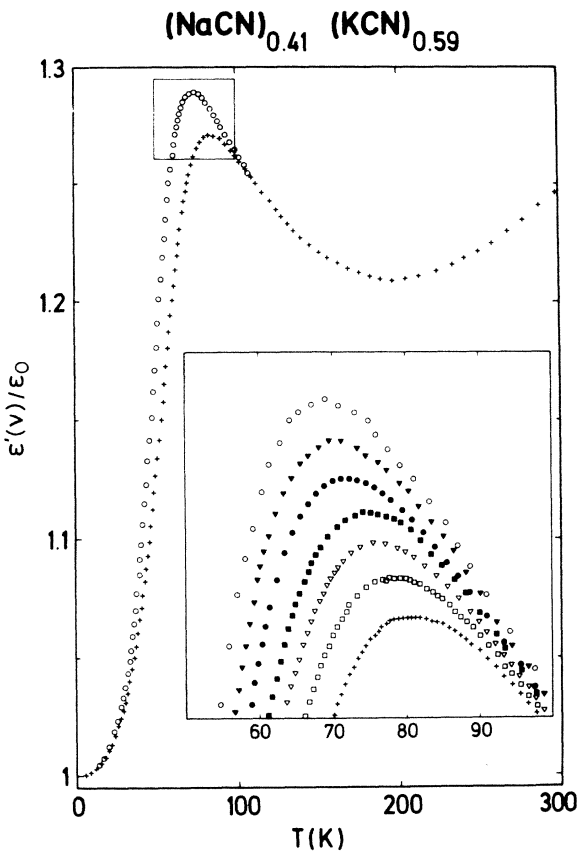

FIG. 12. Normalized real part of the dielectric constant ϵ' for $(NaCN)_{0.41}(KCN)_{0.59}$ versus temperature. ϵ_0 is the dielectric constant $\epsilon'(T\rightarrow 0\ \mathrm{K})=7$ (Ref. 28). The inset shows an enlarged section around the cusp maxima (○, 1 kHz; ▼, 2 kHz; ●, 4 kHz; ■, 10 kHz; ▽, 20 kHz; □, 40 kHz; +, 100 kHz).

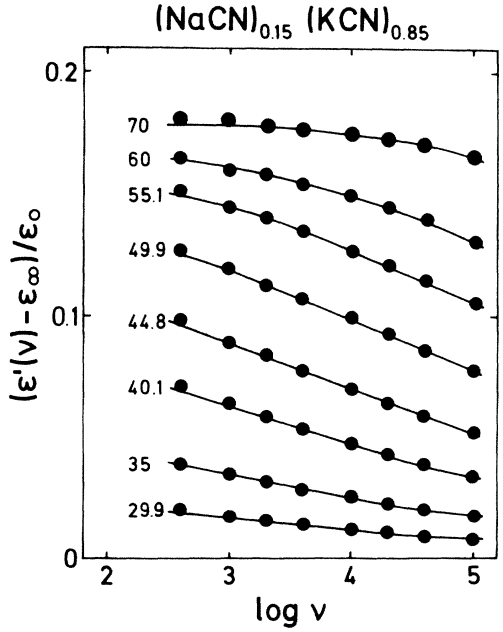

FIG. 13. Normalized dielectric constant $\epsilon'(\nu)$ minus the normalized contributions from the ionic and electronic polarization ϵ_∞ versus $\log_{10}\nu$. ϵ_0 is the dielectric constant $\epsilon'(T\rightarrow 0\ \mathrm{K})=5.8$ (Ref. 28). The solid line is the result of the fit using a symmetric distribution of relaxation times as described in the text.

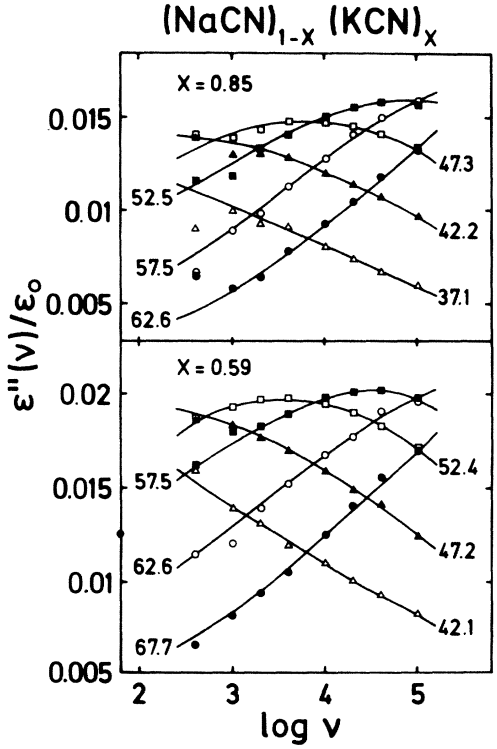

FIG. 14. Normalized imaginary part of the dielectric constant $\epsilon''(\nu)$ versus the logarithm of the measuring frequency in $(NaCN)_{0.15}(KCN)_{0.85}$ (upper half) and $(NaCN)_{0.41}(KCN)_{0.59}$ (lower half) at different temperatures. Differences between experimental and calculated results reflect the limited resolution of the LCR meter at lower frequencies.

Figure 13 demonstrates the frequency dependence of the normalized real part of the dielectric constant in $(NaCN)_{0.15}(KCN)_{0.85}$, where the ionic and electronic contribution ϵ_∞ has been subtracted. ϵ_∞ was assumed to vary with T as in the reference systems KBr and NaBr.[40] Using this procedure, the complex dielectric constant only contains information that originates from the orientational motion of the CN^- dipoles. These data are shown at temperatures where the dispersion effects are important. In both crystals the imaginary part of the dielectric constant $\epsilon''(\nu,T)$ exhibits well-defined, frequency-dependent loss peaks. In Fig. 14 the frequency dependence of ϵ'' is plotted for both crystals investigated at different temperatures. As expected from the smeared-out steps in the real part of the dielectric constants, the loss peaks are rather broad, indicating that the single-particle Debye model is not applicable.

A detailed dielectric investigation of the $(NaCN)_{1-x}(KCN)_x$ system has been performed by Ortiz-Lopez[28] and by Lüty and Ortiz-Lopez.[28] Our results as shown in Figs. 12–14 basically agree with their experimental findings. We mainly were interested in the temperature dependence of the static dielectric susceptibilities to draw some conclusions concerning the dielectric ordering process, bearing in mind that both pure cyanides order antiferroelectrically, namely NaCN at 172 K and KCN at 83 K.

Interactions of the dipoles, whether with the alkali-metal sublattice or with other dipoles, account for a behavior different from the Debye relaxation. The single-particle Debye model predicts a half width of the dielectric loss of about 1.14 decades in frequency and a step in the dielectric constant essentially in the same regime. Several approaches have been developed to treat deviations from the Debye case, namely empirical descriptions utilizing distributions of relaxation times and explanations in terms of a Gaussian distribution of energy barriers. We have chosen the concept introduced by Cole and Cole[41] using a Debye formalism including a symmetric distribution of the relaxation times,

$$\epsilon(\omega)-\epsilon_\infty=\frac{4\pi\chi_s}{1+(i\omega\tau)^{1-\alpha}} . \quad (4)$$

Here, χ_s is the static dielectric susceptibility and τ is the most probable dipolar relaxation time. The temperature dependence of τ can be described using an Arrhenius law:

$$\tau=(2\pi\nu_0)^{-1}\exp\left[\frac{E}{k_BT}\right] . \quad (5)$$

ν_0 is the attempt frequency and E the height of the hindering barrier against dipolar reorientations, i.e., 180° flips. The introduction of the parameter α describes a symmetric broadening of the Debye loss peak and an equivalent smearing out of the dispersion step in the real part of the dielectric constant. The width parameter α can be transformed into the corresponding width W of the dielectric loss via

$$W=2\,\mathrm{arccosh}[2+\sin(\pi\alpha/2)]/(1-\alpha)/\ln(10) . \quad (6)$$

A fit of the real and the imaginary parts of the dielectric constant using Eqs. (3) and (4) gave a good description of the experimental results. The solid lines in Figs. 13 and 14 are the results of these fits. For a given concentration we used a unique set of parameters E and ν_0 to fit the real and imaginary parts of the dielectric constant in the complete temperature range. The hindering barrier E and the attempt frequency ν_0, as determined for both crystals, are given in Table III. In addition, the parameters for KCN and NaCN, as determined from dielectric measurements in the elastically ordered phases (Refs. 28 and 42) and from NMR measurements in the high-temperature disordered phases (Ref. 43), are included.

TABLE III. Dipolar hindering barriers E and attempt frequencies ν_0 in $(NaCN)_{1-x}(KCN)_x$. The parameters for $x=1$ and 0 in the elastically ordered phase (EO) were determined from dielectric measurements by Lüty and Ortiz-Lopez (Ref. 28) and by Lüty (Ref. 42). The data in the pure cyanides in the disordered high-temperature phase (DO) were determined using NMR techniques (Ref. 43).

	E/k_B (K)		ν_0 (Hz)	
x	EO	DO	EO	DO
1	1859	407	1.6×10^{14}	3.7×10^{12}
0.85		1271		2.8×10^{15}
0.59		1677		1.5×10^{17}
0	3254	709	1.6×10^{14}	4.7×10^{12}

The logarithm of the width of the loss peak, W, that corresponds to the Cole-Cole parameter α, is shown in Fig. 15. For both crystals the width of the dielectric loss is much broader than the Debye width and increases with decreasing temperatures. W is significantly larger for $x=0.59$.

Information concerning the static dielectric susceptibility χ_s can be deduced from the dispersion of the real part [$\epsilon'(\nu)-\epsilon_\infty$ for $\nu\to0$] and from the area of the loss peak which is directly related to the static dipolar susceptibility. In addition, at higher temperatures, where the dipolar relaxation rates are much higher than the measuring frequencies, χ_s can be directly deduced from $\epsilon'(T)$ after a suitable background subtraction. The inverse static susceptibility as derived from this analysis is presented in Fig. 16. For $x=0.59$ the complete temperature range ($40<T<175$ K) can be described using a Curie-Weiss law,

$$\chi_s/\epsilon_0=C/(T-\Theta) , \quad (7)$$

with $C=1.9$ K and $\Theta=-30$ K, indicating nearly paraelectric behavior at all temperatures, as expected for weakly interacting dipoles. Thus in $(NaCN)_{0.41}(KCN)_{0.59}$ dipolar interactions can be almost neglected. For $x=0.85$ the inverse static susceptibility χ_s^{-1} behaves radically different, exhibiting only a very slight decrease for $T>70$ K and increasing again at lower temperatures. The high-temperature region can be described with a Curie-Weiss law utilizing the parameters $C=15$ K and $\Theta=-990$ K. These parameters show that antiferroelec-

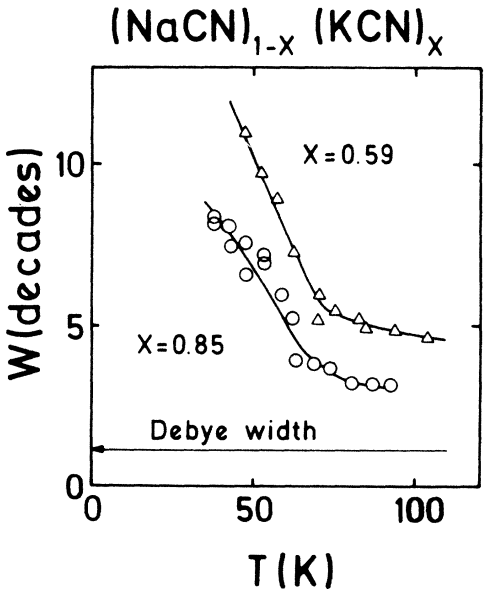

FIG. 15. Logarithm of the full width at half maximum of the dielectric loss W for $(NaCN)_{1-x}(KCN)_x$ mixed crystals with concentrations $x=0.85$ (○) and 0.59 (△). The Debye width $W=1.14$ is also indicated. The solid lines are a guide to the eye only.

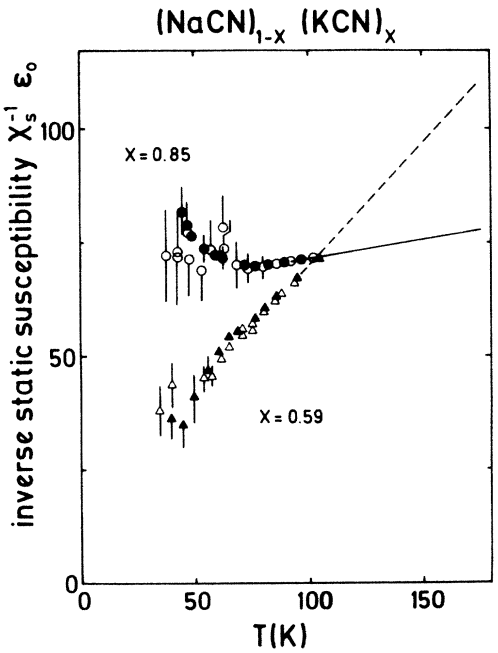

FIG. 16. Normalized inverse static dipolar susceptibility in $(NaCN)_{1-x}(KCN)_x$ for $x=0.85$ (ϕ , $\blacklozenge$) and 0.59 ($\blacklozenge$, $\blacklozenge$) versus temperature. Open symbols: the results of the fits as described in the text using a unique set of parameters for real and imaginary part of the dielectric constant at all temperatures. Solid symbols: best fits allowing for a slight variation of the energy barriers with the temperature. Solid and dashed lines: inverse static susceptibility as calculated at temperatures well above the dispersion regimes. Note that ϵ_0 is slightly different in the two samples: $x=0.85$, $\epsilon'(T\rightarrow 0\text{ K})=5.8$; $x=0.59$, $\epsilon'(T\rightarrow 0\text{ K})=7$ (Ref. 28).

tric interactions play an important role in this crystal. The cusp in χ_s at 70 K is taken as a signal of the onset of dipolar short-range order.[44]

Table III shows that the hindering barriers as determined in the disordered phases in $(NaCN)_{1-x}(KCN)_x$ are considerably higher than in the plastic phases of the pure cyanides, while they are comparable to the hindering barriers as detected in the elastically ordered phases. This indicates that in both crystals investigated locally there are strong deviations from the cubic crystal field. However, the origin of these noncubic crystal fields is different: In $(NaCN)_{0.15}(KCN)_{0.85}$ frozen-in inhomogeneous shear deformations of the cubic lattice create the hindering barriers against dipolar relaxation. In other words, for $x=0.85$ the hindering barriers for dipolar reorientations are due to the quadrupolar interaction forces.[6,39] This is consistent with the results in $(KBr)_{1-x}(KCN)_x$ mixtures, where it has been shown that the dipolar hindering barriers are essentially the same in the elastically ordered and the glassy state.[6] In $(NaCN)_{0.41}(KCN)_{0.59}$ the noncubic crystal field results from the high degree of disturbance introduced by the substitution of the K^+ ions through the Na^+ ions. The high hindering barriers in this sample are the hindering barriers of the single-ion crystalline field which is strongly noncubic. In this case the freezing of the quadrupolar degrees of freedom should have only minor effects on the dipolar relaxation, and the hindering barriers for dipolar and quadrupolar reorientations should be essentially the same.

The attempt frequencies in the potassium cyanide—sodium cyanide mixtures are considerably higher than in the pure cyanides. However, one should be aware that ν_0 and E can be rewritten in terms of a temperature-dependent hindering barrier, giving a linear temperature dependence of E and some reasonable values for the attempt frequencies.[39] This leaves us with some open questions concerning the conclusions in $(NaCN)_{0.41}(KCN)_{0.59}$: If the dipolar freezing is a pure single-ion phenomenon, ν_0 and E should be temperature independent and the attempt frequency is expected to be of the order of the phonon frequencies. In addition, the width of the dielectric loss should also be almost temperature independent, which is not observed experimentally.

III. DISCUSSION

The substitution of potassium ions through smaller sodium ions disturbs the crystal field. Locally, the crystal field becomes highly noncubic, introducing an asymmetry into the reorientational potential, yielding a preferred quadrupolar orientational probability. Only the average over all the CN^- sites exhibits an orientational distribution according to the cubic symmetry of the fcc lattice. The time average of the orientational distribution of a single CN^- ion is strongly noncubic and reflects the asymmetry of the crystal-field potential. The increase of the crystal-field anisotropy with increasing Na^+ concentration can explain the observed dipolar and quadrupolar relaxation kinetics.

A. The quadrupolar freezing process

Analyzing the inelastic-neutron-scattering results, we found that the increase of the crystal-field anisotropy shows up in two effects, namely in a decrease of the rotation-translation coupling and in an increase of the single-particle hindering barrier. The competition between these two effects explains the observed experimental results in $(NaCN)_{1-x}(KCN)_x$. Elastic order is established in the pure cyanides with a dominating rotation-translation coupling; a frozen-in single-ion state appears at low temperatures for mixtures near $x=0.5$, where the coupling to the phonons is weak and the CN^- ions are caught in high hindering barriers of the locally noncubic crystal field. A delicate balance between these two effects yields frozen-in orientational correlations and frozen-in random strains for mixtures near $x=0.2$ and presumably also near $x=0.8$.

B. The dipolar freezing process

From a rigorous analysis of the dipolar slowing down of the molecular motion, we determined the hindering barriers for dipolar reorientations. In both crystals investigated these barrier heights were found to be of comparable size. However, the experimental results indicate that they are created by very different mechanisms: In

$(NaCN)_{0.15}(KCN)_{0.85}$ the barrier heights are mainly determined by frozen-in local strain fields occurring during the quadrupolar freezing process. In $(NaCN)_{0.41}(KCN)_{0.59}$ they are mainly due to the asymmetry of the reorientational potential introduced through the substitution of the K^+ through Na^+ ions. At low temperatures in both crystals, the dipolar relaxation is thus determined by a locally noncubic crystal field, though both are of different origin. Measurements of the dipolar relaxation kinetics above the quadrupolar freezing temperature should yield significant differences: The hindering barriers resulting from strain fields should be decreased for $x=0.85$, while the barriers for $x=0.59$ should be roughly the same above and below T_F as they are given by the chemical disorder.

Similar arguments help to explain the different temperature dependences of the static dipolar susceptibility for $x=0.59$ and 0.85. In $(NaCN)_{0.41}(KCN)_{0.59}$ the easy direction of the crystal field varies from cell to cell. The electric interactions are not strong enough to force any type of electric order, not even on a short scale. In $(NaCN)_{0.15}(KCN)_{0.85}$ the quadrupolar freezing is a cooperative phenomenon. For $T<T_F$ ferroelastic clusters grow in size, giving a distribution of lattice constants. Within these clusters the easy directions in all cells are identical and collinear, and the dipolar interaction forces are strong enough to establish short-range electric order at lower temperatures.

In conclusion, we have investigated the quadrupolar and dipolar susceptibilities in $(NaCN)_{1-x}(KCN)_x$ mixtures. Depending on the concentration x, we found a very different behavior: For $x=0.85$ the quadrupoles undergo a cooperative freezing, establishing a low-temperature glass state with frozen-in orientational correlations and frozen-in lattice strains. At the glass transition from the high-temperature plastic phase to the low-temperature frozen-in state, the onset of orientational correlations destroy the long-range translational order of the center-of-mass lattice. In this crystal the dipolar hindering barriers are created by the quadrupolar interaction forces. At low temperatures short-range electric order can be detected, which is interpreted as antiferroelectric order within the elastically ordered clusters. In $(NaCN)_{0.41}(KCN)_{0.59}$ the quadrupolar relaxation kinetics is determined by the noncubic crystalline field introduced through the alkali-metal substitution and can essentially be described within single-ion behavior. The same crystal-field anisotropy determines the dipolar reorientations.

$(NaCN)_{0.15}(KCN)_{0.85}$ can be characterized as dipolar and quadrupolar glass, where the quadrupolar freezing is the primary relaxation process.

$(NaCN)_{0.41}(KCN)_{0.59}$ exhibits quenched dipolar and quadrupolar disorder at low temperatures. Both freezing processes are essentially single-ion phenomena and should follow the same relaxation behavior.

[1]K. Knorr and A. Loidl, Phys. Rev. B **31**, 5387 (1985).

[2]J. M. Rowe, F. Bouillot, J. J. Rush, and F. Luty, Physica **136B**, 498 (1986).

[3]S. Elschner, K. Knorr, and A. Loidl, Z. Phys. B **61**, 209 (1985).

[4]J. M. Rowe, J. J. Rush, and S. Susman, Phys. Rev. B **28**, 3506 (1983).

[5]J. M. Rowe, J. J. Rush, and E. Prince, J. Chem. Phys. **66**, 5147 (1977).

[6]U. G. Volkmann, R. Böhmer, A. Loidl, K. Knorr, U. T. Höchli, and S. Haussühl, Phys. Rev. Lett. **56**, 1716 (1986).

[7]J. M. Rowe, J. J. Rush, D. J. Hinks, and S. Susman, Phys. Rev. Lett. **43**, 1158 (1980).

[8]A. Loidl, R. Feile, and K. Knorr, Phys. Rev. Lett. **48**, 1263 (1982).

[9]S. K. Satija and C. H. Wang, Solid State Commun. **28**, 617 (1978).

[10]C. W. Garland, J. Z. Kwiecien, and J. C. Damien, Phys. Rev. B **25**, 5818 (1982).

[11]R. Feile, A. Loidl, and K. Knorr, Phys. Rev. B **26**, 6875 (1982).

[12]A. Loidl, R. Feile, and K. Knorr, Z. Phys. B **42**, 143 (1981).

[13]A. Loidl, K. Knorr, R. Feile, and J. K. Kjems, Phys. Rev. Lett. **51**, 1054 (1983); A. Loidl, R. Feile, K. Knorr, and J. K. Kjems, Phys. Rev. B **29**, 6052 (1984).

[14]J. A. Mydosh and G. J. Nieuwenhuys, in *Ferromagnetic Materials*, edited by E. P. Wohlfahrt (North-Holland, Amsterdam, 1980).

[15]J. J. DeYoreo, M. Meissner, R. O. Pohl, J. M. Rowe, J. J. Rush, and S. Susman, Phys. Rev. Lett. **51**, 1050 (1983).

[16]D. Moy, J. N. Dobbs, and A. C. Anderson, Phys. Rev. B **29**, 2160 (1984).

[17]M. Meissner, W. Knaak, J. P. Sethna, K. S. Chow, J. J. DeYoreo, and R. O. Pohl, Phys. Rev. B **32**, 6091 (1985).

[18]J. F. Berret, P. Doussineau, A. Levelut, M. Meissner, and W. Schön, Phys. Rev. Lett. **55**, 2013 (1985).

[19]P. W. Anderson, B. I. Halperin, and C. Varma, Philos. Mag. **25**, 1 (1972).

[20]W. A. Phillips, J. Low Temp. Phys. **7**, 351 (1972).

[21]S. Hunklinger, in *Festkörperprobleme XVII*, edited by J. Treusch (Vieweg, Dortmund, 1977).

[22]K. H. Michel and J. M. Rowe, Phys. Rev. B **22**, 1417 (1980).

[23]J. Ihm, Phys. Rev. B **31**, 1674 (1985).

[24]P. Goldbart and D. Sherrington, J. Phys. C **18**, 1923 (1985).

[25]D. J. Gross, I. Kanter, and H. Sompolinsky, Phys. Rev. Lett. **55**, 304 (1985).

[26]J. P. Sethna and K. S. Chow, Phase Trans. **5**, 317 (1985).

[27]B. Fischer and M. W. Klein, Phys. Rev. Lett. **43**, 289 (1979).

[28]F. Lüty and J. Ortiz-Lopez, Phys. Rev. Lett. **50**, 1289 (1983); J. Ortiz-Lopez, Ph.D. thesis, University of Utah, 1983.

[29]K. H. Michel and J. Naudts, Phys. Rev. Lett. **39**, 212 (1977).

[30]J. M. Rowe, J. J. Rush, N. J. Chesser, K. H. Michel, and J. Naudts, Phys. Rev. Lett. **40**, 455 (1978).

[31]A. Loidl, K. Knorr, J. Daubert, W. Dultz, and W. J. Fitzgerald, Z. Phys. B **38**, 153 (1980).

[32]D. Sahu and S. D. Mahanti, Phys. Rev. B **26**, 2981 (1982).

[33]W. Truthe, Z. Anorg. Chem. **76**, 9 (1912).

[34]A. Loidl, M. Müllner, G. F. McIntyre, K. Knorr, and H. Jex, Solid State Commun. **54**, 367 (1985).

[35]B. D. Silverman, Phys. Rev. Lett. **25**, 107 (1970).

[36]A. Loidl, J. K. Kjems, and S. Haussühl, Z. Phys. B **50**, 187 (1983).

[37]W. Rehwald, J. R. Sandercock, and M. Rossinelli, Phys. Status Solidi A **42**, 699 (1977).

[38]A. Loidl, Habilitationsschrift, Universität Mainz, 1981 (unpublished).

[39]J. P. Sethna, S. R. Nagel, and T. V. Ramakrishnan, Phys.

Rev. Lett. **53**, 2489 (1984).
[40]R. P. Lowndes and D. H. Martin, Proc. R. Soc. London, Ser. A **316**, 351 (1970).
[41]K. S. Cole and R. H. Cole, J. Chem. Phys. **9**, 341 (1941).
[42]F. Lüty, in *Defects in Insulating Crystals,* edited by V. M. Turkevich and K. K. Svarts (Springer-Verlag, Berlin, 1981), pp. 69—89.
[43]S. Elschner and J. Petersson, Z. Phys. B **52**, 37 (1983).
[44]B. Koiller, M. A. Davidovich, and F. Lüty, Phys. Rev. B **31**, 6716 (1985).